Commun Nonlinear Sci Numer Simulat 57 (2018) 388–401

Contents lists available at ScienceDirect

Commun Nonlinear Sci Numer Simulat

journal homepage: www.elsevier.com/locate/cnsns

Research paper

Confidence intervals and hypothesis testing for the Permutation Entropy with an application to epilepsy

Francisco Traversaro [a,b,*], Francisco O. Redelico [c,d]

[a] CONICET - Universidad Nacional de Lanús, Grupo de Investigación en Sistemas de Información, 29 de Septiembre 3901, Lanús, Buenos Aires B1826GLC, Argentina
[b] Instituto Tecnólgico de Buenos Aires (ITBA), Av. Eduardo Madero 399 - (C1181ACH) Ciudad Autónoma de Buenos Aires, Argentina
[c] CONICET - Hospital Italiano de Buenos Aires, Departamento de Informática en Salud, Perón 4190 - (C1199ABB) Ciudad Autónoma de Buenos Aires, Argentina
[d] Universidad Nacional de Quilmes, Departamento de Ciencia y Tecnología, Roque Sáenz Peña 352 - (B1876BXD) Bernal, Buenos Aires, Argentina

ARTICLE INFO

Article history:
Received 18 May 2017
Revised 2 October 2017
Accepted 23 October 2017
Available online 24 October 2017

Keywords:
Permutation Entropy
Epilepsy
Hypothesis test

ABSTRACT

In nonlinear dynamics, and to a lesser extent in other fields, a widely used measure of complexity is the Permutation Entropy. But there is still no known method to determine the accuracy of this measure. There has been little research on the statistical properties of this quantity that characterize time series. The literature describes some resampling methods of quantities used in nonlinear dynamics - as the largest Lyapunov exponent - but these seems to fail. In this contribution, we propose a parametric bootstrap methodology using a symbolic representation of the time series to obtain the distribution of the Permutation Entropy estimator. We perform several time series simulations given by well-known stochastic processes: the $1/f^{\alpha}$ noise family, and show in each case that the proposed accuracy measure is as efficient as the one obtained by the frequentist approach of repeating the experiment. The complexity of brain electrical activity, measured by the Permutation Entropy, has been extensively used in epilepsy research for detection in dynamical changes in electroencephalogram (EEG) signal with no consideration of the variability of this complexity measure. An application of the parametric bootstrap methodology is used to compare normal and pre-ictal EEG signals.

1. Introduction

In 2002, Bandt and Pompe introduced a measure of complexity for time series [1] named *permutation entropy* (PE). It is an information entropy [2] that takes account of the time evolution of the time series, in contrast with other prominent information entropies as the Shannon entropy [3]. Its computation is fast, requires not too long time series [4], it is robust against noise [5] and distributional assumptions of the time series [6]. This measure has been widely used in non-linear dynamics [7–11], and to a lesser extent in Stochastic Processes [12–14], among others. It has also had a great impact on such different and important areas of applied science and engineering as varied as Mechanics Engineering [15,16], Epilepsy

* Corresponding author at: Instituto Tecnólgico de Buenos Aires (ITBA), Av. Eduardo Madero 399 - (C1181ACH) Ciudad Autónoma de Buenos Aires, Argentina.
E-mail address: francisco.redelico@hospitalitaliano.org.ar (F. Traversaro).

https://doi.org/10.1016/j.cnsns.2017.10.013
1007-5704/

[17,18], Anesthesia [19], Cardiology [20,21], Finance [22], Climate Change [23]. Also a book about Permutation Complexity has been published [24].

Since its publication and up to the end of 2016, the Bandt and Pompe seminal work [1] has been cited in 789 papers, according Scopus bibliographic database, and the evolution of the cites seems to indicate that it will be increasing within time. All these facts made an investigation of PE from the statistic point of view an important issue.

There has been little research, up to our knowledge, on the statistical properties of the quantities used in nonlinear dynamics to characterize time series. This lack of research may be due the lack of distributional theory of these quantities, yielding resampling techniques as the most powerful tool to overcome this task. Perhaps one exception to this is the research on the distribution of the largest Lyapunov exponent and the correlation dimension [25]. In [26] a methodology to calculate the empirical distributions of Lyapunov exponents based on a traditional bootstrapping technique is presented, providing a formal test of chaos under the null hypothesis. However, in [27] it is shown that the previously bootstrap approach seems to fail to provide reliable bounds for the estimates of the Lyapunov's exponents, and conclude that the traditional bootstrap cannot be applied for estimating multiplicative ergodic statistics. In [28], a moving blocks bootstrap procedure is used to detect a positive Lyapunov exponent in financial time series. However, the time series generated by moving block bootstrap present artifacts which are caused by joining randomly selected blocks, so the serial dependence is preserved within, but not between, the blocks.

Regarding time series symbolic dynamics, in [29] the probabilities generated using the Bandt and Pompe methodology are calculated analytically for Gaussian Processes for motiv length equal three, but they recognize that for larger lengths this is not possible, and for that reason a computer based method is required to estimate the bias and variance in the PE estimation.

In this contribution we propose a different simulation method (i.e. parametric bootstrap) for estimating the bias, variance and confidence intervals for the Permutation Entropy estimation, along with hypothesis testing, that consists in simulating symbolic time series bootstrap samples that are thought to be produced by a probabilistic model with a fixed transition probability extracted from the original time series.

In order to show some results from our method we simulate a well known family of time series: the $1/f^{\alpha}$ noise. We compute bias, variance and confidence intervals for the Permutation Entropy of these time series according to the time series length along with other parameters. In addition, an application of the parametric bootstrap methodology for hypothesis testing is used to compare normal and pre-ictal EEG signals.

The paper reads as follows: Section 2 shows a brief review of PE in order to present the estimator to be evaluated using the bootstrap approach, Section 3 presents and explains the proposed parametric bootstrap, firstly a brief review of the bootstrap scheme is done as an introduction to our method, then in Section 3.1 the core of this bootstrap approach is presented, i.e. the probability transitions computation, and finally in Section 3.2 the algorithms to perform the parametric bootstrap of PE is explained. Section 4 addresses the numerical simulation along with its results, in Section 5 an application of the parametric bootstrap is used to compare normal and pre-ictal EEG signals and Section 6 is devoted to the conclusions of this contribution.

2. Permutation Entropy

In this Section, we briefly review the PE to make the article self-contained and accessible for a wider audience.

Let $\{X_t\}_{t\in T}$ be a realization of a data generator process in form of a real valued time series of length $T \in \mathbb{N}$. A measure of uncertainty about $\{X_t\}_{t\in T}$ is the *normalized* Shannon entropy [3] ($0 \leq \mathcal{H} \leq 1$), which is defined as:

$$\mathcal{H}[P] \;=\; S[P]/S_{max} \;=\; \left\{-\sum_{i=1}^{N} P_i \;\ln(P_i)\right\}/S_{max}, \tag{1}$$

where P_i is a probability to be extracted from the time series, N is the cardinality of the P_i set $\{p_i\}_1^N$, the denominator $S_{max} = S[P_e] = \ln N$ is obtained by a uniform probability distribution $P_e = \{P_i = 1/N,\ \forall i = 1, \cdots, N\}$.

Bandt and Pompe proposed a symbolization technique to estimate P_i and compute PE, $\hat{\mathcal{H}}(m, \tau)$. First, we recall that PE has two tuning parameters, i.e. m the symbol length and τ the time delay. Within this paper, we set $\tau = 1$ with no loss of generality and it will be omitted, so we will use $\mathcal{H} = \mathcal{H}(m)$ for sake of simplicity. Let $X_m(t) = (x_t, x_{t+1}, \ldots, x_{t+m-1})$ with $0 \leq t \leq T - m + 1$ be a non-disjoint partition containing the vectors of real values of length m of the time series $\{X_t\}_{t\in T}$. Let $S_{m\geq 3}$ the symmetric group of order $m!$ formed by all possible permutations of order m, $\pi_i = (i_1, i_2, \ldots, i_m) \in S_m$ ($i_j \neq i_k \forall j \neq k$ so every element in π_i is unique). We will call an element π_i in S_m a symbol or a motiv as well. Then $X_m(t)$ can be mapped to a symbol π_i in S_m for a given but otherwise arbitrary t. The m real values $X_m(t) = (x_t, x_{t+1}, \ldots, x_{t+m-1})$ are mapped onto their rank. The rank function is defined as:

$$R(x_{t+n}) = \sum_{k=0}^{m-1} \mathbb{1}(x_{t+k} \leq x_{t+n}) \tag{2}$$

where $\mathbb{1}$ is the indicator function (i.e $\mathbb{1}(Z) = 1$ if Z is true and 0 otherwise), $x_{t+n} \in X_m(t)$ with $0 \leq n \leq m-1$ and $1 \leq R(x_{t+n}) \leq m$. So the rank $R(min(x_{t+k})) = 1$ and $R(max(x_{t+k})) = m$. The complete alphabet is all the possible permutations

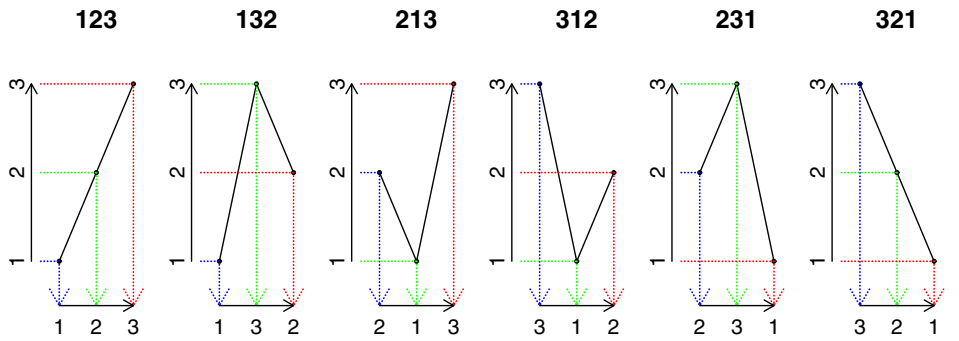

Fig. 1. All symbols for $m = 3$ are shown. With this rank permutation mapping one simply maps each value x_i in $X_m(t)$ placing its rank $R(x_i) \in \{1, 2, \ldots, m\}$ in chronological order to form π_i in S_m. The indexes of the vertical axis are fixed, ordered by amplitude (i.e ranks), and they are mapped onto the time axis. For each pattern $X_3(t) = (x_t, x_{t+1}, x_{t+2})$, the resultant symbol can be obtained reading the labels in the horizontal axis from left to right (in chronological order).

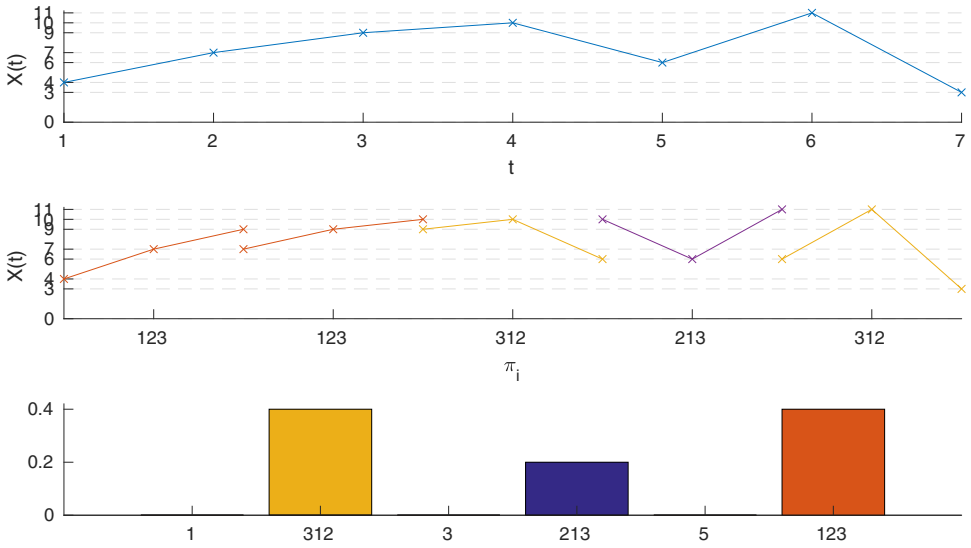

Fig. 2. Example of the calculation of the Permutation Entropy. (top) Time series $X_t = (4, 7, 9, 10, 6, 11, 3)$. (middle) symbols π_i generated from the time series using the Rank Permutation Mapping. (bottom) relative frequency of $S_{m=3}$ elements for the exemplified time series, $P(312) = 0.4$, $P(123) = 0.4$ and $P(213) = 0.2$.

of the ranks. Hence, any vector $X_m(t)$ is uniquely mapped onto $\pi_i = (R(x_t), R(x_{t+1}), \ldots, R(x_{t+m-1})) \in S_m$. With this Rank Permutation Mapping one simply maps each value x_i in $X_m(t)$ placing its rank $R(x_i) \in \{1, 2, \ldots, m\}$ in chronological order to construct π_i in S_m. In Fig. 1 an illustrative drawing of this mapping for all the alternatives in $m = 3$ is presented. The indexes of the vertical axis are fixed, ordered by amplitude (i.e ranks), and they are mapped onto the time axis. The resultant symbol can be obtained reading the labels in the horizontal axis from left to right (in chronological order). This method is used by Bandt [30], Riedl et al. [4] and Bandt and Shiha [31] among others. For example, let us take the series with seven values ($T = 7$) used in [1] (see Fig. 2, top), and motiv length $m = 3$:

$$X_t = (4, 7, 9, 10, 6, 11, 3) \tag{3}$$

$X_3(1) = (4, 7, 9)$ and $X_3(2) = (7, 9, 10)$ represents the permutation $\pi = 123$ since $R(x_1) = 1$,$R(x_2) = 2$, $R(x_3) = 3$. $X_3(3) = (9, 10, 6)$ and $X_3(4) = (6, 11, 3)$ correspond to the permutation $\pi = 231$ since $R(x_1) = 2$,$R(x_2) = 3$, $R(x_3) = 1$ (see Fig. 2, middle). Using the rank permutation Mapping we compute $P(\pi_i)$ (see Fig. 2, bottom),

$$P(\pi_i) = \frac{\sum_{l=1}^{T-m+1} \mathbb{1}(X_m(l) \text{ has ordinal patter } \pi_i \text{ in } S_m)}{T - m + 1}, \tag{4}$$

where $\mathbb{1}$ is the indicator function and $i = 1, \ldots, m!$. Using these probabilities, $\hat{\mathcal{H}}(m)$ can be computed as,

$$\hat{\mathcal{H}}(m) = \left\{ -\sum_{i=1}^{N} P(\pi_i) \ \ln(P(\pi_i)) \right\} / S_{max}, \tag{5}$$

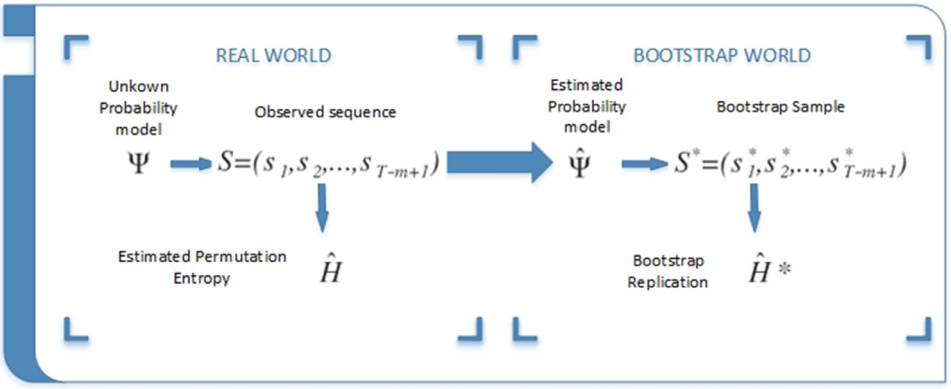

Fig. 3. Schematic diagram of the parametric bootstrap approach. An unknown probability model, $\Psi = \Psi(P^{ij})$, gives an observed sequence S from which we estimate $\hat{\mathcal{H}}$, so the bootstrap approach suggest to estimate this model $\hat{\Psi} = \Psi(\hat{P}^{ij})$ and get the correspondent bootstrap samples S^* from which we estimate $\hat{\mathcal{H}}^*$.

where $N = m!$ is the order of the symmetric group S_m and $S_{max} = ln(N)$.

3. The bootstrap approach

The bootstrap is a computer based method for assigning measures of accuracy to the estimates of the desired statistical variables [32]. If $\mathcal{H}$ is an unknown characteristic of a model Ψ, an estimator $\hat{\mathcal{H}}$ can be derived from the sample generated by Ψ in a single experiment. A way to obtain the distribution of $\hat{\mathcal{H}}$ is to repeat the experiment a large number of times and approximate the distribution of $\hat{\mathcal{H}}$ by the so obtained empirical distribution. In most practical situations, this method is impossible because the experiment is not reproducible, or is unenforceable for cost reasons. The spirit of the bootstrap methodology is to estimate the sampling distribution of a statistic (i.e. quantifier or a parameter estimator) from the data at hand by analogy to the "thought experiment" that motivates the sampling distribution.

Suppose that an unknown probability model Ψ gives an observed data set $\mathbf{X} = \{x_t\}_{t=1}^{n}$ by random sampling and let $\hat{\theta}_{\Psi}(\mathbf{X}, T)$ be the statistic of interest that estimates our true value $\theta = f(\Psi)$. Then with the observed data set $\mathbf{X}$ we produce an estimate $\hat{\Psi}$. The trick is now to repeat the random sampling but with the estimate $\hat{\Psi}$ giving bootstrap samples $\mathbf{X}^* = \{x_t^*\}_{t=1}^{n}$ and for each bootstrap sample we calculate $\hat{\theta}^*_{\hat{\Psi}}(\mathbf{X}^*, n)$. Now we repeat the bootstrap sampling B times and the distribution of $\hat{\theta}^*_{\hat{\Psi}}(\mathbf{X}^*, n)$ is the bootstrap estimator of the distribution of $\hat{\theta}_{\Psi}(\mathbf{X}, n)$. With this estimated distribution we can also obtain the variance, the bias and the confidence intervals of our estimator.

Formally, the bootstrap methodology is based in the plug-in principle [33]. The parameter of interest can be written as a function of the probability model, $\theta = f(\Psi)$. As the probability model is unknown, the plug-in estimate of our parameter is defined to be $\hat{\theta} = f(\hat{\Psi})$. So the bootstrap propose that we resample from this estimated probability model $\hat{\Psi}$ that is chosen to be close to Ψ in some sense.

If we have some information about Ψ besides the data, the chosen $\hat{\Psi}$ must contain this information. Suppose that we know that the data $\mathbf{X} = \{x_t\}_{t=1}^{n}$ comes from a certain process ruled by a probabilistic model Ψ that depends on a finite number of parameters $\Xi = \{\xi\}_{i=1}^{k}$, so $\Psi = f(\Xi)$. This parameters can be estimated in the traditional statistical parametric approach as Maximum Likelihood getting $\hat{\Xi} = \{\hat{\xi}\}_{i=1}^{k}$, and equivalently $\hat{\Psi} = f\left(\hat{\xi}\right)$.

Now the bootstrap samples $\mathbf{X}^* = \{x_1^*, x_2^* \dots x_n^*\}$ comes from a process ruled by a probabilistic model $\hat{\Psi}$ (Fig. 3). These bootstrap samples emulates in every sense the original samples, including the correlation between the values.

3.1. The transition probabilities of a symbol sequence

As stated in Section 2 using the methodology proposed by Bandt and Pompe, the dynamics of a process $\{X_t\}_{t\in T}$ with $X_t \in \mathbb{R}$ is represented by a $m!$th finite state random process $\{S_t\}_{t\in(T-m+1)}$ with $S_t \in S_m = \{\pi_1, \pi_2 \dots \pi_{m!}\}$ for all possible $m \geq 2$. This realization of the symbolic sequence is thought to be produced by a probabilistic model with a fixed transition probability P^{ij} (i.e. the probability of moving from a symbol π_i to a symbol π_j for all $1 \leq i \leq m!$ and $1 \leq j \leq m!$) denoted $\Psi(P^{ij})$.

As seen in Fig. 3 $\Psi = \Psi(P^{ij})$, gives an observed sequence S from which we estimate $\hat{\mathcal{H}}$, so we need an estimation of the $\hat{P}^{ij}$ to estimate the model $\hat{\Psi} = \Psi(\hat{P}^{ij})$ in order to obtain bootstrap replications $\hat{\mathcal{H}}^*$.

According to Bandt and Pompe [1], the relative frequency

$$\hat{P}_T(\pi_i) = \frac{n_i}{T - m + 1} \tag{6}$$

is an estimate *as good as possible for a finite series of values* of $P(\pi_i)$, with n_i the number of times the state π_i is observed up to time $T-m+1$. The sub-index T in $\hat{P}_T(\pi_i)$ reinforces the notion of the dependence of the estimator on the length of the series T.

With the same spirit, we define the transition probabilities of the symbol sequence as:

$$P^{ij} = P(s_{t+1} = \pi_j | s_t = \pi_i) \quad 1 \leq i \leq j \leq m! \tag{7}$$

And the estimator of P^{ij}

$$\hat{P}_T^{ij} = \begin{cases} \frac{n_{ij}}{n_i} & if\ n_i \geq 0 \\ 0 & otherwise \end{cases} \tag{8}$$

where n_{ij} is the number of transitions observed form π_i to π_j up to time $T-m+1$ and n_i the number of times the state π_i is observed up to time $T-m+1$. Note $n_i = \hat{P}(\pi_i)(T-m+1)$

Then by the law of the total probability:

$$P(\pi_j) = \sum_{i=1}^{m!} P(\pi_i) P^{ij} \tag{9}$$

so if we call $\mathbf{P}(\pi)$ to the (m!)-dimensional vector containing $P(\pi_i)$ in each coordinate (i.e $\mathbb{P}(\pi) = (P(\pi_1), P(\pi_2), \ldots, P(\pi_{m!}))$, then $\mathbf{P}(\pi)$ is determined by P^{ij}, leading to the conclusion that the estimator $\hat{\mathbf{P}}_T(\pi)$ is determined by the estimation of $\hat{P}_T^{ij}$.

3.2. Bootstrapping the Permutation Entropy

The Permutation Entropy is defined in Eq. (1), so because of the plug-in principle, our natural estimator is:

$$\hat{\mathcal{H}}_T = \left\{ -\sum_{i=1}^{N} \hat{P}_T(\pi_i) \ln(\hat{P}_T(\pi_i)) \right\} / ln(m!) \tag{10}$$

In Section 3.1 we showed that the Permutation Entropy was completely defined by the transition probabilities P^{ij} so we can think of them as parameters of a probabilistic model Ψ.

Following the scheme in Fig. 3 we have:

$\Psi\left(P^{ij}\right) \longrightarrow \mathbf{S} = (s_1, s_2 \ldots, s_{T-m+1}) \longrightarrow \hat{\mathcal{H}}_T$

Our probabilistic model with unknown transition probabilities P^{ij} gives the observed symbol sequence $\mathbf{S}$, and with that sequence the estimation of the Permutation Entropy is obtained.

In the "bootstrap world":

$\hat{\Psi} = \Psi\left(\hat{P}_T^{ij}\right) \longrightarrow \mathbf{S}^* = (s_1^*, s_2^* \ldots, s_{T-m+1}^*) \longrightarrow \hat{\mathcal{H}}_T^*$

$\hat{\Psi}$ generates $\mathbf{S^*}$ by a simulation, giving the bootstrap replication $\hat{\mathcal{H}}_T^*$. We can repeat the simulation to get as many bootstrap replications as affordable.

Computing B bootstrap replication of the Permutation Entropy from a time series $\{X_t\}_{t\in T}$ is simple: given a time series of length T, choose a world length m and a time delay τ to do the mapping from $\{X_t\}_{t\in T}$ to $\{S_t\}_{t\in(T-m+1)}$ as stated in Section 2. With this sequence: compute $\hat{P}_T(\pi_i)$, (Eq. (6)), $\hat{P}_T^{ij}$ (Eq. (8)) and calculate $\hat{\mathcal{H}}_T$ (Eq. (10)). Then choose at random with probability $\hat{P}_T(\pi)$ an initial state $s_1^*(b) = \pi_k$ and choose at random with probability $\hat{P}_T^{kj}$ (note that k is fixed with the value of the previous state) the next simulated state $s_2^*(b)$. Repeat this last step $T-m+1$ times to obtain the simulation $\mathbf{S}^*(\mathbf{1}) = (s_1^*(1), s_2^*(1) \ldots, s_{T-m+1}^*(1))$. With this bootstrap replication of symbol sequence estimate $\hat{\mathcal{H}}_T^*(b)$ (Eq. (6)).

For a more detailed reference see Algorithm 1 in Appendix A.

Repeat the simulation of the sequence B times to obtain $\hat{H}_T^*(b) \quad b = 1 \ldots B$. With the set $\hat{\mathcal{H}}_T^*(b) \quad b = 1 \ldots B$ we have the bootstrap replications needed to estimate the standard deviation, the confidence intervals of $\hat{\mathcal{H}}_T$, or the test presented in the following section.

Now, with the B obtained bootstrap replications of $\hat{\mathcal{H}}_T^*$:

$\hat{\mathcal{H}}_T^*(1), \hat{\mathcal{H}}_T^*(2) \ldots \hat{\mathcal{H}}_T^*(B)$

The Bootstrap Standard Deviation of $\hat{\mathcal{H}}_T^*$ is our estimation of the Standard Deviation of $\hat{\mathcal{H}}_T$:

$$\hat{\sigma}_B(\hat{\mathcal{H}}_T) = \hat{\sigma}(\hat{\mathcal{H}}_T^*) \tag{11}$$

and is defined as

$$\hat{\sigma}(\hat{\mathcal{H}}_T^*) = \sqrt{\frac{1}{B-1} \sum_{i=1}^{B} \left(\hat{\mathcal{H}}_T^*(i) - \hat{\mathcal{H}}_T^*(\bullet)\right)^2} \tag{12}$$

where

$$\hat{\mathcal{H}}_T^*(\bullet) = \frac{1}{B} \sum_{i=1}^{B} \hat{\mathcal{H}}_T^*(i) \tag{13}$$

We define the bootstrap bias of $\hat{\mathcal{H}}_T^*$ as:

$$\text{Bias}(\hat{\mathcal{H}}_T^*) = \hat{\mathcal{H}}_T^*(\bullet) - \hat{\mathcal{H}}_T \tag{14}$$

Finally, the Mean Square Error (MSE) of an estimator:

$$\text{MSE}(\hat{\mathcal{H}}_T^*) = Var(\hat{\mathcal{H}}_T^*) + Bias^2(\hat{\mathcal{H}}_T^*) \tag{15}$$

3.2.1. Confidence intervals

The $1-\alpha$ Confidence Interval of $\mathcal{H}$ is defined by the percentiles of the bootstrap δ. For each bootstrap replicate $\hat{\mathcal{H}}_T^*(b)$ we compute the difference - $\delta^*(b)$ - between that replication and the mean of all bootstrap replicates. Then we choose the $(\frac{\alpha}{2})$ and the $(1-\frac{\alpha}{2})$ percentiles of the δ^*'s distribution and add them to the original estimate, $\hat{\mathcal{H}}_T^*$, correcting for the bias, and the resulting $(1-\alpha)100\%$ confidence interval is:

$$\left[\max(2\hat{\mathcal{H}}_T - \hat{\mathcal{H}}_T^*(\bullet) + \delta^*_{\frac{\alpha}{2}}, 0), \min(2\hat{\mathcal{H}}_T - \hat{\mathcal{H}}_T^*(\bullet) + \delta^*_{(1-\frac{\alpha}{2})}, 1)\right] \tag{16}$$

For a more detailed reference see Algorithm 2 in Appendix A.

3.2.2. Hypothesis testing

With this same spirit, a confidence interval for the difference between the Permutation Entropy of two different time series can be made. In inferential statistics exists a direct relationship between confidence intervals and hypothesis testing. A two-sided $(1-\alpha)$ confidence interval in the difference between two measures can be used to determine if those two measures are significantly different by only checking if the *zero* belongs to this particular interval.

$H_0 : \Delta = \mathcal{H}_1 - \mathcal{H}_2 = 0$

If $0 \notin (1-\alpha)100\%\ CI\ (\Delta)$ then reject H_0 and

$$\mathcal{H}_1 \neq \mathcal{H}_2$$

The procedure to perform this test is shown in Algorithm 3 in Appendix A.

4. Numerical simulation

In order to show our proposed bootstrap in a very general time series, we simulate a well known dynamical system: the $1/f^\alpha$. All the series are simulated with different time span -*T*- in order to evaluate the statistical properties of $\hat{\mathcal{H}}_T$ according to Eq. (10). As stated before, a way to obtain the distribution of $\hat{\mathcal{H}}$ is to repeat the experiment a large number of times and approximate the distribution of $\hat{\mathcal{H}}$ by the so obtained empirical distribution. While for real world experiments this can be inapplicable, for simulated time series this can easily done by Monte Carlo Simulation. Once the n replications of $\hat{\mathcal{H}}_T = \{\hat{\mathcal{H}}_T(1), \ldots, \hat{\mathcal{H}}_T(n)\}$ is obtained the standard deviation is estimated by:

$$\hat{\sigma}(\hat{\mathcal{H}}_T) = \sqrt{\frac{1}{n-1}\sum_{i=1}^{n}\left(\hat{\mathcal{H}}_T(i) - \hat{\mathcal{H}}_T(\bullet)\right)^2} \tag{17}$$

where

$$\hat{\mathcal{H}}_T(\bullet) = \frac{1}{n}\sum_{i=1}^{n}\hat{\mathcal{H}}_T(i) \tag{18}$$

4.1. Experimental design

$1/f^\alpha$ noises refers to a signal with spectral density $S(f)$ with the form $S(f) = k\frac{1}{f^\alpha}$ where k is a constant, α is the signal-dependent parameter and f is frequency [34]. It is a stochastic model which seems to be ubiquitous in nature (see [34] and the references within). We simulate $1/f^\alpha$ noises with $\alpha = \{-1, 0, 1, 2\}$. See Fig. 4 for an example of these noises. A *white noise* process ($\alpha = 0$) would generate a curve with constant power in the spectrum. The case of $\alpha = 1$ or *pink noise* is the canonical case and of most interest as many of the values of α found in nature are very near to 1.0 [35–39]. A random walk noise (Brownian Motion or *red noise*, $\alpha = 2$) would show a $(1/f^2)$ distribution in $S(f)$. In order to simulate this stochastic process, the algorithm propose in [40] is used.

For each $\alpha = \{-1, 0, 1, 2\}$ 1000 replications were simulated for each $T = \{60,\ 100,\ 120,\ 400,\ 600,\ 2000,\ 3600,\ 5000,\ 10,000,\ 20,000,\ 50,000\}$. $\hat{\mathcal{H}}_i(T, m)$ for $\{i = 1 \ldots 1000\}$ along with $\hat{\sigma}(\hat{\mathcal{H}}_T)$ are obtained for $m = \{3, 4, 5, 6\}$. For each $\alpha = \{-1, 0, 1, 2\}$ a single replication was simulated for each $T = \{60,\ 100,\ 120,\ 400,\ 600,\ 2000,\ 3600,\ 5000,\ 10,000, 20,000, 50,000\}$. In each case for this replication we implemented the Algorithm 1 to get 1000 bootstrap replicates. $\hat{\mathcal{H}}_i^*(T, m)$ for $\{b = 1 \ldots 1000\}$ are obtained for $m = \{3, 4, 5, 6\}$. For these bootstrap samples we analyze *Bias, Standard Deviation* and *MSE*.

As for each set of 1000 bootstrap replicates we obtain a single confidence interval, we repeated this step 50 times to obtain Table 1 that indicates the estimated confidence level of this method along with the mean amplitude of the interval.

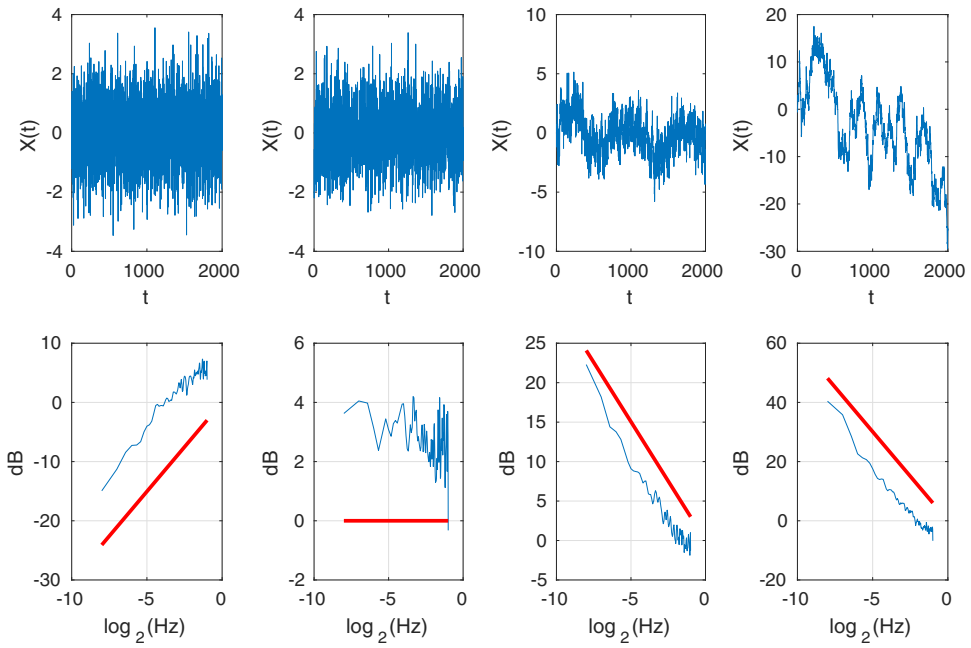

Fig. 4. (top) realization for $1/f^k$ noises (T = 2000), from left to right: $k = -1, k = 0, k = 1, k = 2$. (bottom) spectral density of the respective $1/f^k$ noises.

Table 1
90% Confidence Intervals (Eq. (16)) for every symbol length m and power law parameter α. How many times the real value of $\mathcal{H}$ (in fact we use the mean of $\hat{\mathcal{H}}(T, m)$ that is the best possible estimator) is lower than the Lower Bound -*MissLeft*- or higher than the Upper Bound -*MissRight*-. For white noise the confidence level is higher than 90%, in fact is always accurate but for other values of α the overall confidence level is approximately between 90% and 95%.

m	α	$\hat{\mathcal{H}}(T, m)$	MissLeft	MissRight	Mean amplitude
3	−1	0.995831848	0	0.04	0.00222
4	−1	0.989083439	0.02	0.04	0.00420
5	−1	0.983495069	0.04	0.04	0.00500
6	−1	0.97547007	0.02	0	0.00555
3	0	0.99990292	0	0	0.00057
4	0	0.999679839	0	0	0.00080
5	0	0.998800463	0	0	0.00134
6	0	0.994503528	0	0	0.00235
3	1	0.991622896	0.02	0.02	0.00340
4	1	0.983385433	0.02	0.02	0.00493
5	1	0.97600538	0.02	0.04	0.00591
6	1	0.966355927	0	0.06	0.00657
3	2	0.943233315	0.08	0.06	0.00959
4	2	0.90634703	0.04	0.02	0.01273
5	2	0.878452628	0.02	0.02	0.01413
6	2	0.853327039	0.04	0.02	0.01482

4.2. Results

We intend to show in our simulated experiment that the bootstrap distribution of the PE estimator is close in every meaningful sense to the distribution obtained by the repetition of the original experiment (empirical distribution) when the exact replication of the experiment can not be done. A comparison between the standard deviations of both bootstrap replicates and the empirical distribution ($\hat{\sigma}_B(\hat{\mathcal{H}}_T)$ and $\hat{\sigma}(\hat{\mathcal{H}}_T)$ respectively) for the stochastic processes is presented in Fig. 5. There are some discrepancies for low values of T but from a certain value T_0, in all the cases of m, the standard deviation coincides. In Fig. 6 it can be seen that for every m and α the bias of the bootstrap estimate tends to zero as T increases. So, the estimator of the PE is an asymptotically unbiased estimator. With this and with the fact that σ also goes to zero as T increases, the estimation seems to be Mean Square Consistent. Even more, for large values of T, the estimation is as efficient as the estimation produced by the repetition of the experiment. In Fig. 7 and for an arbitrary value of $\alpha = 1$ an for the largest length of the simulated time series $T = 50,000$, an histogram of the bootstrap estimator along with an histogram of the simulated estimator are presented in different scale for every m. The similar shape between the histograms can be

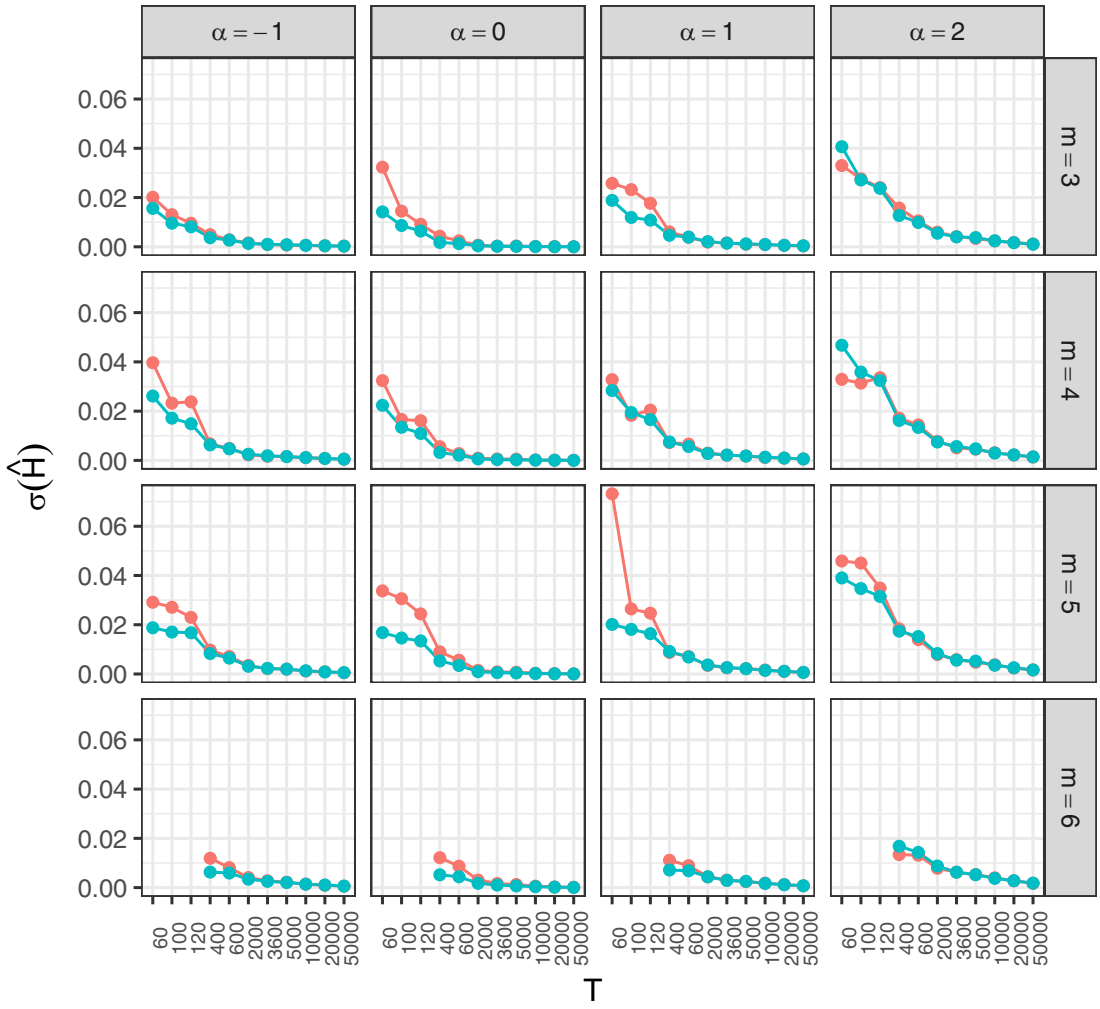

Fig. 5. Standard Deviation of $\hat{\mathcal{H}}$ as T increases. A comparison between the standard deviations of $\hat{\mathcal{H}}$ of both bootstrap replicates in red and simulated replicates in blue is shown. There are some discrepancies for low values of T but form a certain value T_0, in all the cases of symbol length m and α, the standard deviation coincide. As the bias goes to zero (Fig. 6) along with the standard deviation the PE estimator seems to be a mean square consistent estimator. (For interpretation of the references to color in this figure legend, the reader is referred to the web version of this article.)

appreciated, the difference in the location is due that the bootstrap samples depends on only one of the estimations of the PE (that are random) but this does not affect the posterior inferential conclusions.

For a more thorough exploration of the bootstrap estimator we have calculated fifty 90% Confidence Intervals and for every m and every α we computed how many times the real value of $\mathcal{H}$ - in fact we use the mean of $\hat{\mathcal{H}}(T, m)$ (see Section 4.1) that is the best possible estimator - is outside the bounds of the confidence interval. Results are shown in Table 1. For white noise the confidence level is higher than 90% (in fact is always accurate) but for other values of α the overall confidence level is approximately between 90% and 95%.

5. Application: EEG data

To illustrate the proposed confidence intervals in real contexts we present how it can describe the uncertainty in the Permutation Entropy estimation within one observation of Electroencephalogram (EEG) Data. More precisely, as a first practical application, we analyze four different sets of EEGs for healthy and epileptic patients that were previously analyzed by Andrzejak et al. [41] (available at http://www.meb.unibonn.de/epileptologie/science/physik/eegdata.html). The data consist of 100 data segments (from which we choose 10 at random), whose length is 4097 data points with a sampling frequency of 173.61 Hz, of brain activity for different groups and recording regions: surface EEG recordings from five healthy volunteers in an awake state with eyes open (Set A) and closed (Set B), intra-cranial EEG recordings from five epilepsy patients during the seizure free interval from outside (Set C) and from within (Set D) the seizure generating area. Details about the recording technique of these EEG data can be found in the original paper.

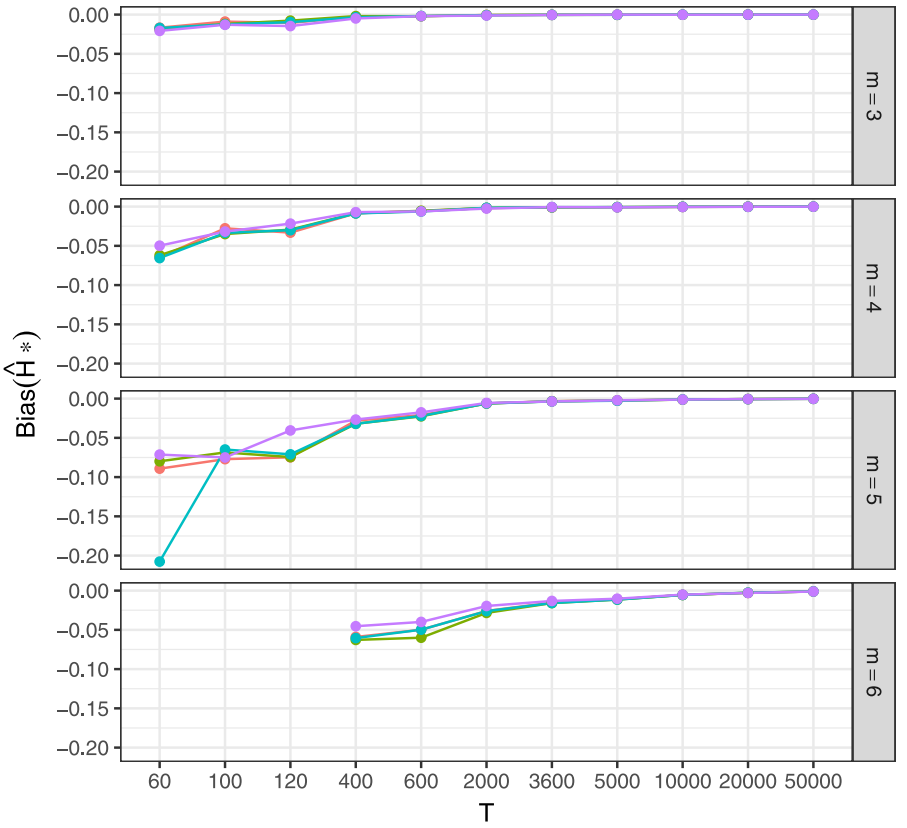

Fig. 6. The Bootstrap Bias for different values of α in function of T. It can be seen that for every symbol length m and α the bias of the bootstrap estimate tends to zero as T increases. The PE estimator is an asymptotically unbiased estimator. As the standard deviation goes to zero (Fig. 5) along with the bias the PE estimator seems to be a mean square consistent estimator.

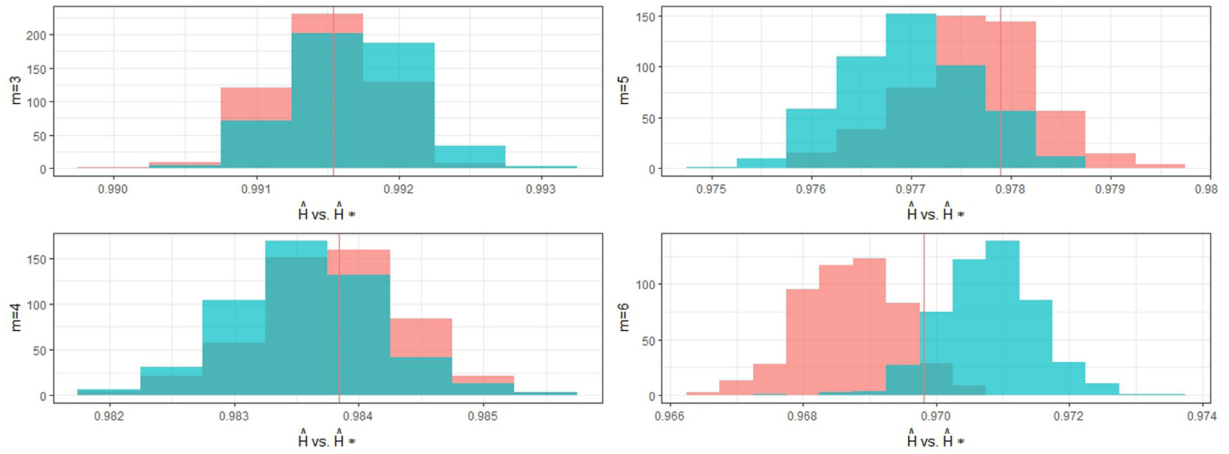

Fig. 7. For an arbitrary value of $\alpha = 1$ an for the largest length of the simulated time series $T = 50,000$, an histogram of the bootstrap estimator (Red) along with an histogram of the simulated estimator (Blue) are presented in different scales for every m. The similar shape between the histograms can be appreciated, the difference in the location is due that the bootstrap samples depends on only one of the estimations of the PE (that are random) but this does not affect the posterior inferential conclusions. (For interpretation of the references to color in this figure legend, the reader is referred to the web version of this article.)

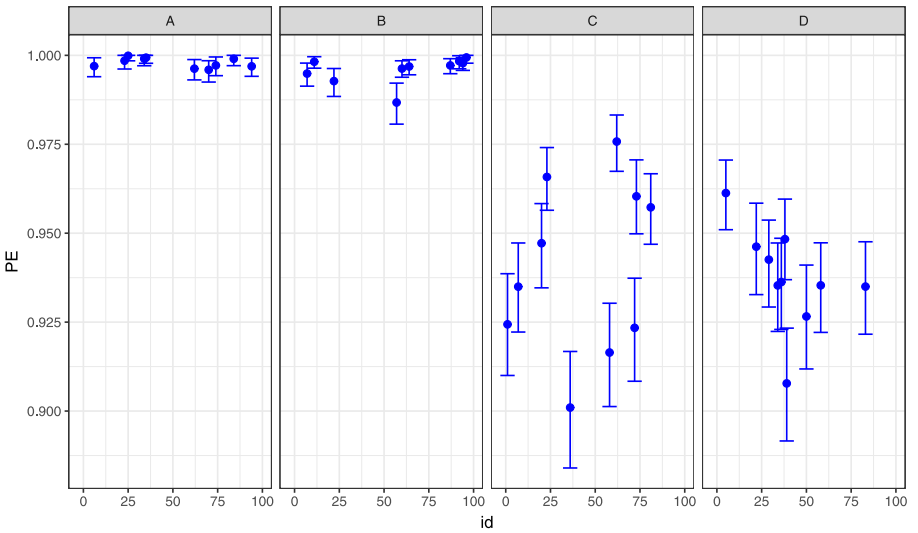

Fig. 8. The 90% Confidence Intervals for the 10 EEG signals of brain activity for different groups and recording regions: surface EEG recordings from healthy volunteers in an awake state with eyes open (Set A) and closed (Set B), intra-cranial EEG recordings from epilepsy patients during the seizure free interval from outside (Set C) and from within (Set D) the seizure generating area. It should be pointed out that the overlapping between intervals does not necessarily means that there is no significant differences between the two Permutation Entropies. To reach that conclusion, an hypothesis test for the difference must be made.

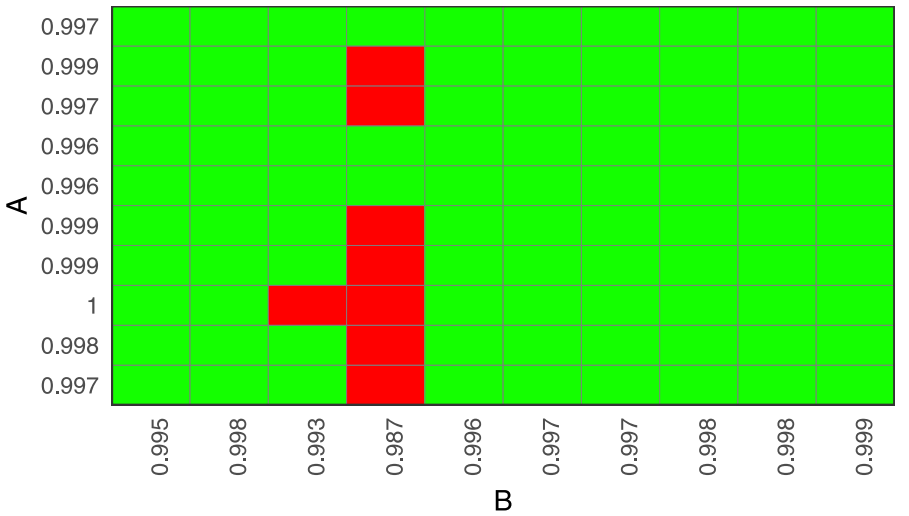

Fig. 9. Hypothesis Test for the difference in the Permutation Entropy of a time series. A test for the difference in the Permutation Entropy between the EEG signals of healthy volunteers in an awake state with eyes open (Set A, in rows) and the EEG signals of healthy volunteers in an awake state with eyes closed (Set B, in columns). In order to obtain an overall significance of 0.1 ($\alpha = 0.1$) for the 100 tests performed in the analysis, each individual test for the difference between the PE of a single EEG of the Set A and a single EEG of the Set B (each square) was conducted with a significance level of 0.001 ($\alpha = 0.001$). The red squares mean that the individual test was rejected and there is a significant difference between the Permutation Entropies. On the other side green squares mean that the individual test was not rejected and there is no evidence for that difference. 8 individual tests were rejected out of 100 indicating that there were differences between Set A and Set B, but 7 of these rejected tests belong to the same patient with eyes closed who may have been affected by an external factor. (For interpretation of the references to color in this figure legend, the reader is referred to the web version of this article.)

The problem of interest is to compare, via an inferential procedure, the PE of 4 different sets of EEG signals: EEG signals of patients in an awake state with eyes open (Set A) and closed (Set B), intra-cranial EEG recordings from epilepsy patients during the seizure free interval from outside (Set C) and from within (Set D) the seizure generating area.

The classical approach to this problem is sampling several EEG signals of each type, and conduct a test of comparison between means with the *t*-test if normality holds, or through a Mann Whitney–Wilcoxon test if no assumption of the distribution of the PE were made. Multiple comparisons can be made with an ANOVA and a posterior Tukey HSD test, or with

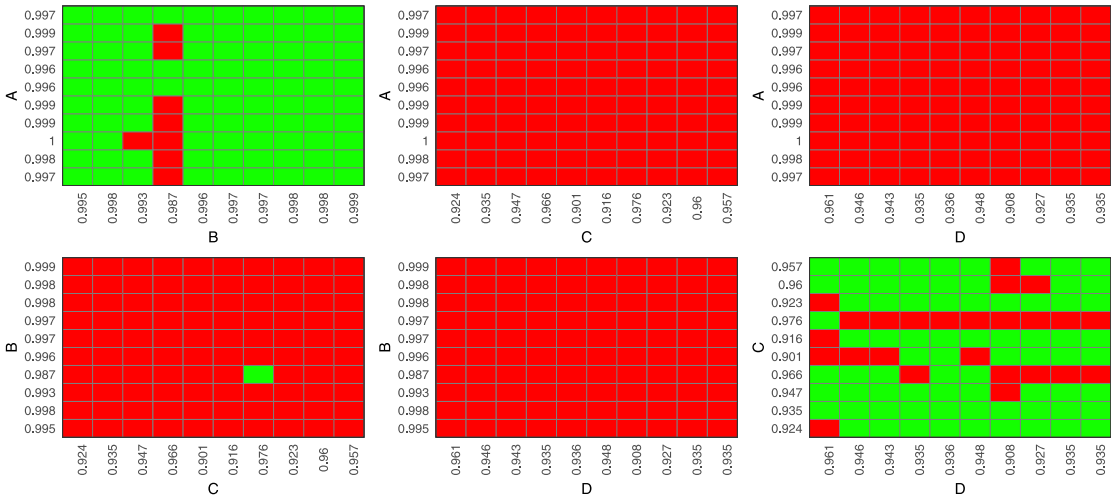

Fig. 10. The same analysis of the previous figure is extended to all the different types of patients. All the global tests indicates that there were differences between different Sets, but between Set A and Set B the difference is mostly due a single patient (who may have been affected by an external factor) and all EEG signals of those sets are different in every test to the EEG signals of Set C and Set D, except for one. Instead, between Set C and Set D the differences between the individuals are distributed between significant and not significant.

the equivalent non-parametric test, the Kruskal–Wallis test by ranks. With this approach one can draw conclusions about the relation between the means of the PE of the EEG signals of the different sets, but cannot compare the dynamics (via the PE) between individual EEG signals of those different sets. With the bootstrap approach presented on this contribution, one can establish if any EEG signal in a Set A, for example, is significantly different (in the PE) to any signal in Set B. And then repeat this procedure between all the sets. We begin by constructing 90% Confidence Intervals for the PE of the 10 EEG signals of brain activity for different groups and recording regions (Fig. 8) in order to visualize the location of the PE estimator along with its variability. It should be pointed out that the overlapping between intervals does not necessarily means that there is no significant differences between the two Permutation Entropies [42]. To reach that conclusion, an hypothesis test for the difference must be made.

Next we perform a test for the difference in the Permutation Entropy between the EEG signals of healthy volunteers in an awake state with eyes open (Set A, in rows) and the EEG signals of healthy volunteers in an awake state with eyes closed (Set B, in columns), see Fig. 9. In order to obtain an overall significance of 0.1 ($\alpha = 0.1$) for the 100 tests performed in the analysis, each individual test for the difference between the PE of a single EEG of the Set A and a single EEG of the Set B (each square) was conducted with a significance level of 0.001 ($\alpha = 0.001$). 8 individual tests were rejected out of 100 indicating that there were differences between Set A and Set B, but 7 of these rejected tests belong to the same patient with eyes closed who may have been affected by an external factor.

In Fig. 10 the same analysis is extended to all the different types of patients. All the global tests indicates that there were differences between different Sets, but between Set A and Set B the difference is mostly due a single patient (who may have been affected by an external factor) and all EEG signals of those sets are different in every test to the EEG signals of Set C and Set D, except for one. Instead, between Set C and Set D the differences between the individuals are distributed between significant and not significant.

6. Conclusion

The repetition of the "thought experiment" that produces the data to calculate the statistic $\hat{\mathcal{H}}$ is the basis of obtaining the distribution. The infinite repetition of this experiment would give the actual distribution, so a large number of this repetitions should be the best estimator of the distribution of the statistic $\hat{\mathcal{H}}$. In real world applications is very often impossible to repeat the experiment, so performing an analogy of this experiment using the data at hand is the purpose of bootstrap. In many practical situations, there is a wish to compare the dynamics of two processes via the Permutation Entropy of their time series. The question is: $\mathcal{H}_1 = \mathcal{H}_2$? This can not be answered with punctual estimators $(\hat{\mathcal{H}}_1, \hat{\mathcal{H}}_2)$ because these are continuous random variables and with probability 1 (i.e. *always*) they are going to be different. The real question is if that difference is statistically significant or not, and that only can be answered if a measure of variability exists for that continuous random variable, $\hat{\Delta} = \hat{\mathcal{H}}_1 - \hat{\mathcal{H}}_2$. There has not been, up to our best knowledge, this kind of variability measure that we are proposing now.

With the bootstrap estimator of the variance and bias that we present in this contribution, the PE is an asymptotically unbiased estimator and seems to be Mean Square Consistent. Even more, for large values of T, the proposed accuracy measure is as efficient as the one obtained by the frequentist approach of repeating the experiment.

In summary, we present a computer based methodology to obtain an accuracy measure for the estimation of the Permutation Entropy ($\hat{\mathcal{H}}$). So far we found in the literature that only descriptive statistics are used to characterize this quantifier and if the objective is to reach conclusions that extend beyond the raw data itself, there were no statistical inference method at hand. Even a simple comparison between two random variables (as $\hat{\mathcal{H}}$) cannot be made with some confidence without a measure of variability of that variable. Our method paves the way to perform any inferential statistic involving the Permutation Entropy or even any complexity measure that uses the Probability Function Distribution proposed by Bandt and Pompe.

Appendix A. Algorithms

Algorithm 1 Algorithm for the parametric bootstrap for Permutation Entropy.

$T \leftarrow$ time series length
set m
set τ
compute $\hat{P}_T(\pi_i)$ (Eq. (6)) from the actual time series
compute $\hat{\mathcal{H}}_T$ (Eq. (10)) from the actual time series
compute $\hat{P}_T^{ij}$ (Eq. (8)) from the actual time series
$b \leftarrow 1$
while $b \leq B$ **do**
  $i \leftarrow 1$
  $s_i^*(b) \leftarrow \pi_k$ w.p. $\hat{P}_T(\boldsymbol{\pi})$ {i. e. the initial state for the bth bootstrap replication}
  while $i \leq T - m + 1$ **do**
    $s_{(i+1)}^*(b) \leftarrow \pi_k$ w.p. $\hat{P}_T^{ik}(\boldsymbol{\pi})$ {i. e. the ith state for the bth bootstrap replication}
    $i \leftarrow i + 1$
  end while
  estimate $\hat{P}^*(\boldsymbol{\pi})$ using $\mathbf{S}^*(b)$ Ec. 7
  estimate $\hat{\mathcal{H}}_T^*(b)$ using $\hat{P}^*(\boldsymbol{\pi})$ and Ec. 11 {i. e. the b bootstrap sample of $\hat{\mathcal{H}}_T$.}
end while

Algorithm 2 Algorithm for the confidence interval for Permutation Entropy.

while $b \leq B$ **do**
  generate $\hat{\mathcal{H}}_T^*(b)$
end while
compute $\hat{\mathcal{H}}_T^*(\bullet) = \frac{1}{B}\sum_{i=1}^{B} \hat{\mathcal{H}}_T^*(i)$
sort $\delta^*(b) = \hat{\mathcal{H}}_T^*(b) - \hat{\mathcal{H}}_T^*(\bullet)$ in increasing order
set confidence level $1 - \alpha$
compute $\delta^*_{\frac{\alpha}{2}} \leftarrow \left\{ \delta^*_{\frac{\alpha}{2}} \Big/ \frac{\#\left(\delta^* < \delta_{\frac{\alpha}{2}}\right)}{B} \leq \frac{\alpha}{2} \right\}$
{i. e. if $B = 1000$ and $\alpha = 0.1$ choose the 50th element on the sorted δ^* }
compute
$\delta^*_{(1-\frac{\alpha}{2})} \leftarrow \left\{ \delta^*_{(1-\frac{\alpha}{2})} \Big/ \frac{\#\left(\delta^* < \delta_{(1-\frac{\alpha}{2})}\right)}{B} \leq 1 - \frac{\alpha}{2} \right\}$
{i. e. if $B = 1000$ and $\alpha = 0.1$ choose the 950th element on the sorted δ^* }
The lower bound of the confidence interval is
$\max(2\hat{\mathcal{H}}_T - \hat{\mathcal{H}}_T^*(\bullet) + \delta^*_{\frac{\alpha}{2}}, 0)$
The upper bound of the confidence interval is
$\min(2\hat{\mathcal{H}}_T - \hat{\mathcal{H}}_T^*(\bullet) + \delta^*_{(1-\frac{\alpha}{2})}, 1)$

Algorithm 3 Algorithm for the hypothesis testing for Permutation Entropy.

compute $\hat{\mathcal{H}}_{1T}$ the PE of the 1st time series
compute $\hat{\mathcal{H}}_{2T}$ the PE of the 2nd time series
compute $\hat{\Delta}_T = \hat{\mathcal{H}}_{1T} - \hat{\mathcal{H}}_{2T}$
while $b \leq B$ **do**
  generate $\hat{\mathcal{H}}_{1T}^{*}(b)$ the bootstrap replicate of the 1st time series
  generate $\hat{\mathcal{H}}_{2T}^{*}(b)$ the bootstrap replicate of the 2nd time series
end while
for i in 1 to B **do**
  for k in 1 to B **do**
    compute $\Delta_T^*(n) = \hat{\mathcal{H}}_{1T}^{*}(i) - \hat{\mathcal{H}}_{2T}^{*}(k)$
  end for
end for
compute $\hat{\Delta}_T^*(\bullet) = \frac{1}{B^2}\sum_{i=1}^{B^2} \hat{\Delta}_T^*(n)$
sort $\delta^*(n) = \Delta_T^*(n) - \hat{\Delta}_T^*(\bullet)$ in increasing order
set confidence level $1-\alpha$
compute $\delta^*_{\frac{\alpha}{2}} \leftarrow \left\{ \delta^*_{\frac{\alpha}{2}} \Big/ \frac{\#\left(\delta^* < \delta_{\frac{\alpha}{2}}\right)}{B} \leq \frac{\alpha}{2} \right\}$
{i. e. if $B = 1000$ and $\alpha = 0.1$ choose the 50th element on the sorted δ^* }
compute
$\delta^*_{(1-\frac{\alpha}{2})} \leftarrow \left\{ \delta^*_{(1-\frac{\alpha}{2})} \Big/ \frac{\#\left(\delta^* < \delta_{(1-\frac{\alpha}{2})}\right)}{B} \leq 1-\frac{\alpha}{2} \right\}$
{i. e. if $B = 1000$ and $\alpha = 0.1$ choose the 950th element on the sorted δ^* }
The lower bound of the confidence interval is
$\hat{\Delta}_T + \delta^*_{\frac{\alpha}{2}}$
The upper bound of the confidence interval is
$\hat{\Delta}_T + \delta^*_{(1-\frac{\alpha}{2})}$
If 0 does not belong to the interval
Then $\mathcal{H}_1 \neq \mathcal{H}_2$ with α level of signification.

References

[1] Bandt C, Pompe B. Permutation entropy: a natural complexity measure for time series. Phys Rev Lett 2002;88(17):174102.
[2] Gray RM. Entropy and information theory. Springer Science & Business Media; 2011.
[3] Shannon CE. A mathematical theory of communication. ACM SIGMOBILE Mobile Comput Commun Rev 2001;5(1):3–55.
[4] Riedl M, Müller A, Wessel N. Practical considerations of permutation entropy. Eur Phys J Spec Top 2013;222(2):249–62.
[5] Quintero-Quiroz C, Pigolotti S, Torrent M, Masoller C. Numerical and experimental study of the effects of noise on the permutation entropy. New J Phys 2015;17(9):093002.
[6] Traversaro F, F R. Characterization of autoregressive processes using entropic quantifiers. Physica A 2017.
[7] Keller K, Sinn M. Ordinal analysis of time series. Physica A 2005;356(1):114–20.
[8] De Micco L, González C, Larrondo H, Martin M, Plastino A, Rosso O. Randomizing nonlinear maps via symbolic dynamics. Physica A 2008;387(14):3373–83.
[9] Rosso OA, De Micco L, Larrondo HA, Martín MT, Plastino A. Generalized statistical complexity measure. Int J Bifurcation Chaos 2010;20(03):775–85.
[10] Masoller C, Rosso OA. Quantifying the complexity of the delayed logistic map. Philos Trans R Soc London A 2011;369(1935):425–38.
[11] Zanin M, Zunino L, Rosso OA, Papo D. Permutation entropy and its main biomedical and econophysics applications: a review. Entropy 2012;14(8):1553–77.
[12] Rosso O, Zunino L, Pérez D, Figliola A, Larrondo H, Garavaglia M, et al. Extracting features of gaussian self-similar stochastic processes via the bandt-pompe approach. Phys Rev E 2007;76(6):061114.
[13] Sinn M, Keller K. Estimation of ordinal pattern probabilities in gaussian processes with stationary increments. Comput Stat Data Anal 2011;55(4):1781–90.
[14] Zunino L, Pérez D, Martín M, Garavaglia M, Plastino A, Rosso O. Permutation entropy of fractional brownian motion and fractional gaussian noise. Phys Lett A 2008;372(27):4768–74.
[15] Yan R, Liu Y, Gao RX. Permutation entropy: a nonlinear statistical measure for status characterization of rotary machines. Mech Syst Signal Process 2012;29:474–84.
[16] Redelico FO, Traversaro F, Oyarzabal N, Vilaboa I, Rosso OA. Evaluation of the status of rotary machines by time causal information theory quantifiers. Physica A 2017;470:321–9.
[17] Redelico FO, Traversaro F, García MdC, Silva W, Rosso OA, Risk M. Classification of normal and pre-ictal eeg signals using permutation entropies and a generalized linear model as a classifier. Entropy 2017;19(2):72.
[18] Olofsen E, Sleigh J, Dahan A. Permutation entropy of the electroencephalogram: a measure of anaesthetic drug effect. Br J Anaesth 2008;101(6):810–21.
[19] Jordan D, Stockmanns G, Kochs EF, Pilge S, Schneider G. Electroencephalographic order pattern analysis for the separation of consciousness and unconsciousnessan analysis of approximate entropy, permutation entropy, recurrence rate, and phase coupling of order recurrence plots. J Am Soc Anesthesiologists 2008;109(6):1014–22.
[20] Frank B, Pompe B, Schneider U, Hoyer D. Permutation entropy improves fetal behavioural state classification based on heart rate analysis from biomagnetic recordings in near term fetuses. Med Biol Eng Comput 2006;44(3):179.

[21] Parlitz U, Berg S, Luther S, Schirdewan A, Kurths J, Wessel N. Classifying cardiac biosignals using ordinal pattern statistics and symbolic dynamics. Comput Biol Med 2012;42(3):319–27.
[22] Matilla-García M, Marín MR. Detection of non-linear structure in time series. Econ Lett 2009;105(1):1–6.
[23] Carpi LC, Saco PM, Figliola A, Serrano E, Rosso OA. Analysis of an el nino-southern oscillation proxy record using information theory quantifiers. In: Concepts and recent advances in generalized information measures and statistics; 2013. p. 3.
[24] Amigó J. Permutation complexity in dynamical systems: ordinal patterns, permutation entropy and all that. Springer Science & Business Media; 2010.
[25] Boeing G. Visual analysis of nonlinear dynamical systems: chaos, fractals, self-similarity and the limits of prediction. Systems 2016;4(4):37.
[26] Gençay R. A statistical framework for testing chaotic dynamics via lyapunov exponents. Physica D 1996;89(3–4):261–6.
[27] Ziehmann C, Smith LA, Kurths J. The bootstrap and lyapunov exponents in deterministic chaos. Physica D 1999;126(1):49–59.
[28] Brzozowska-Rup K, Orłowski A. Application of bootstrap to detecting chaos in financial time series. Physica A 2004;344(1):317–21.
[29] Bandt C, Shiha F. Order patterns in time series. J Time Ser Anal 2007;28(5):646–65.
[30] Bandt C. Autocorrelation type functions for big and dirty data series. ArXiv e-prints2014;.
[31] Bandt C, Shiha F. Order patterns in time series. J Time Ser Anal 2007;28(5):646–65.
[32] Efron B, Tibshirani R. Bootstrap methods for standard errors, confidence intervals, and other measures of statistical accuracy. Stat Sci 1986:54–75.
[33] Efron B, Tibshirani RJ. An introduction to the bootstrap. New York: Chapman & Hall; 1993.
[34] Kasdin NJ. Discrete simulation of colored noise and stochastic processes and $1/f^{\alpha}$ power law noise generation. Proc IEEE 1995;83(5):802–27.
[35] Caloyannides M. Microcycle spectral estimates of 1/f noise in semiconductors. J Appl Phys 1974;45(1):307–16.
[36] Kobayashi M, Musha T. 1/f fluctuation of heartbeat period. IEEE Trans Biomed Eng 1982(6):456–7.
[37] Novikov E, Novikov A, Shannahoff-Khalsa D, Schwartz B, Wright J. Scale-similar activity in the brain. Phys Rev E 1997;56:R2387–9. doi:10.1103/PhysRevE.56.R2387.
[38] Voss RF, Clarke J. 1/fnoise'in music and speech. Nature 1975;258:317–18.
[39] Dutta P, Horn P. Low-frequency fluctuations in solids: 1 f noise. Rev Mod Phys 1981;53(3):497.
[40] Timmer J, Koenig M. On generating power law noise.. Astron Astrophys 1995;300:707.
[41] Andrzejak RG, Lehnertz K, Mormann F, Rieke C, David P, Elger CE. Indications of nonlinear deterministic and finite-dimensional structures in time series of brain electrical activity: Dependence on recording region and brain state. Phys Rev E 2001;64(6):061907.
[42] Payton ME, Greenstone MH, Schenker N. Overlapping confidence intervals or standard error intervals: what do they mean in terms of statistical significance? J Insect Sci 2003;3(1):34.